

Evaluation of Grooving Corrosion and Electrochemical Properties of H₂S Containing Oil/Gas Transportation Pipes Manufactured by Electric Resistance Welding

Maksudur Rahman¹, Siva Prasad Murugan¹, Changwook Ji², Yong Jin Cho³,
Joo-Yong Cheon², and Yeong-Do Park^{1,†}

¹Department of Advanced Materials Engineering, Dong-Eui University, Busan, 47340, Korea

²Advanced Forming Process R&D Group, KITECH, Ulsan, 44413, Korea

³Ship Infrared Signature Research Center, Department of Naval Architecture and Ocean Engineering, Dong-Eui University, Busan, 47340, Korea

(Received April 09, 2018; Revised May 16, 2018; Accepted June 15, 2018)

Electrical Resistance Welding (ERW) on a longitudinal seam-welded pipe has been extensively used in oil and gas pipelines. It is well known that the weld zone commonly suffers from grooving corrosion in ERW pipes. In this paper, the grooving corrosion performances of API X65 grade non-sour service (steel-A) and API X70 grade sour gas resistant (steel-B) steel electrical resistance welding pipelines were evaluated. The microstructure of the bondline is composed of coarse polygonal ferrite grains and several elongated pearlites. The elongated pattern is mainly concentrated in the center of the welded area. The grooving corrosion test and electrochemical polarization test were conducted to study the corrosion behavior of the given materials. A V-shaped corrosion groove was found at the center of the fusion zone in both the steel-A and steel-B ERW pipes, as the corrosion rate of the bondlines is higher than that of the base metal. Furthermore, the higher volume fraction of pearlite at the bondline was responsible for the higher corrosion rate at the bondline of both types of steel.

Keywords: Electrical resistance welding, Grooving corrosion, Seam welding, Bondline, API X65

1. Introduction

Electrical Resistance Welding (ERW) is a controlled high precision welding process in which seam welding of steel pipes are formed by High Frequency Induction Heating (HFI) process. ERW longitudinal seam-welded pipe has been used in many applications including oil and gas pipelines, heat exchangers, water pipelines, and construction (e.g., scaffolding). Weld zone and base metal have electrochemical potential differences that causes corrosion problems ERW pipes [1]. Grooving corrosion, in which the weld suffers V-shaped selective corrosion, will occur in the fusion zone. This grooving corrosion is critical since it shortens the life of ERW steel pipes not only due to penetration that leads to leaks but also because the defect that tends to be formed during grooving corrosion is similar to a long, sharp notch which can act as the initiation site for fatigue and environmentally assisted

cracking [2]. The resistance of ERW pipes to grooving corrosion can be improved by adding some alloying elements such as Cu, Ca, Ni, Nb, Ti to the steel. In order to control the grooving corrosion of ERW steel pipes, the relationship between grooving corrosion, chemical composition, and steel microstructure needs to be better understood. In the present study, a constant potential polarization approach is used to investigate the performances of grooving corrosion of X65 grade Non-Sour Service and X70 grade Sour gas resistant steel pipelines and comparisons are made between them.

2. Experimental Methods

Two different kinds of steel pipes, namely steel-A and steel-B were used for this investigation. The chemical composition of the materials is provided in the Table 1. Fig. 1 shows the Schematic diagram of the ERW process [3]. After the pipe was shaped from the sheet, it was welded by ERW technology. The welding conditions of ERW pipes are given in the Table 2. Annealing was done just

[†] Corresponding author: ypark@deu.ac.kr

Table 1 Chemical composition of the materials

	C	Si	Mn	P	S	Ti	V	Nb	Cr	Ni
Steel-A	0.06	0.23	1.46	0.009	0.001	-	-	-	-	-
Steel-B	0.02	0.26	1.3	0	0	-	0.04	0.05	0.19	0.08

Table 2 Welding conditions of ERW pipes

Materials	Thickness	Welding speed	Welding power	Welding power per thickness
Steel-A	9.2 mm	15.0 m/min	185 kW	20.12 kW/mm
Steel-B	12.0 mm	11.5 m/min	297kW	24.75 kW/mm

after the ERW welding at 900 °C.

The tested of pipes were cut from different manufacturing positions which are shown in Fig. 2. All pieces had dimensions of 9.2 – 12 mm thick depending on the thickness of the pipes, 15 mm long, and 10 mm wide. The weld was parallel to the direction of the specimen’s width, located in the center of the specimen’s width, and was across the specimen’s thickness. The curved sides were machined smooth and were then ground with 100 – 1000 grit emery paper prior to testing. The final specimen thickness was measured with an accuracy of ± 0.001 mm for calculating the corrosion depth. The inner surfaces of the ERW pipes were taken as the test surfaces and other surfaces are sealed. Then the specimens were exerted at

20mA/cm² current and polarized for 20 hours in a 3.5 wt% NaCl aqueous solution at room temperature to accelerate the grooving corrosion. Illustration of electrodes system used in grooving corrosion test is shown in Fig. 3. The specimen of the ERW pipe was used as an anode. The corroded specimen was cross-sectioned through the weld or the corrosion groove and the cut surface was ground with 100 – 1000 grit emery paper. After testing, any corrosion products were removed and parameters of grooving corrosion were measured by following Zongyue Bi *et al.* [3] according to Fig. 4. The grooving corrosion sensitivity coefficient, α , is defined as

$$\alpha = \frac{h_2}{h_1} \tag{1}$$

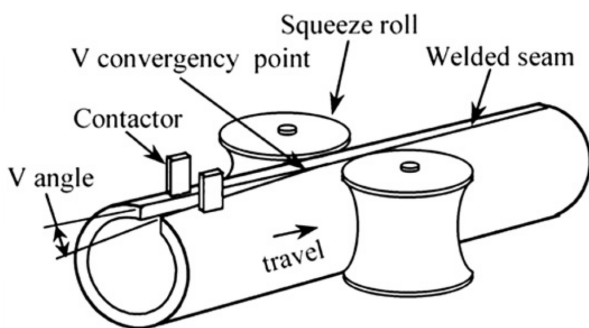


Fig. 1 Schematic diagram of the ERW process [16].

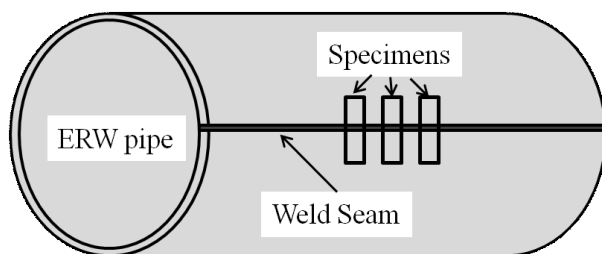


Fig. 2 Schematic diagram of Specimens cutting positions.

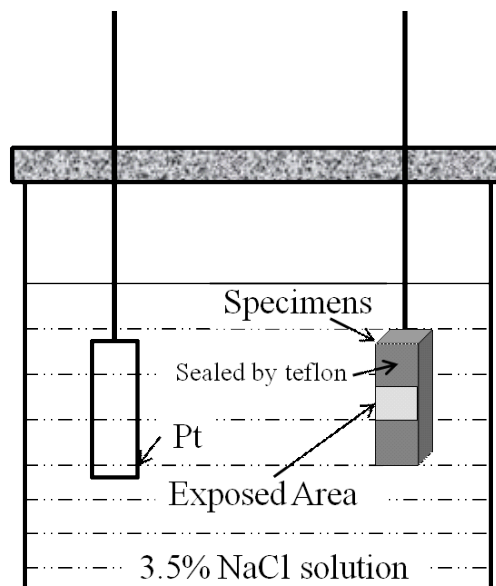


Fig. 3 Illustration of electrodes system used in grooving corrosion test (bondline remains at the center of the exposed area).

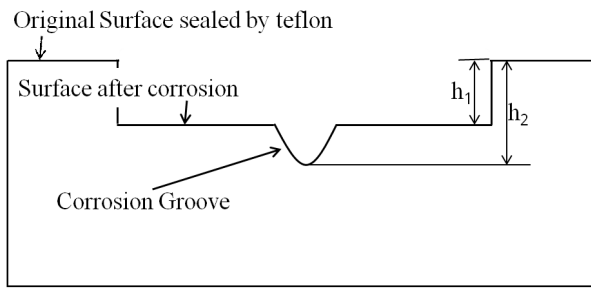


Fig. 4 Illustration of determining sensitivity coefficient of grooving corrosion.

	Steel-A	Steel-B
Corrosion groove formation in 3.5% NaCl atmosphere for 48 hours and 20 mA/cm ²		
G.F. (α)	1.322	1.104
B.W. (μm)	100.9	68.7

Fig. 5 Corrosion groove, grooving factor(G.F.- α) and bond-line width (B.W.) of steel-A and steel-B.

Where h_2 and h_1 are the depths from origin surface to corrosion groove base and corrosion depth of base metal respectively. h_1 is equal to the difference between the orig-

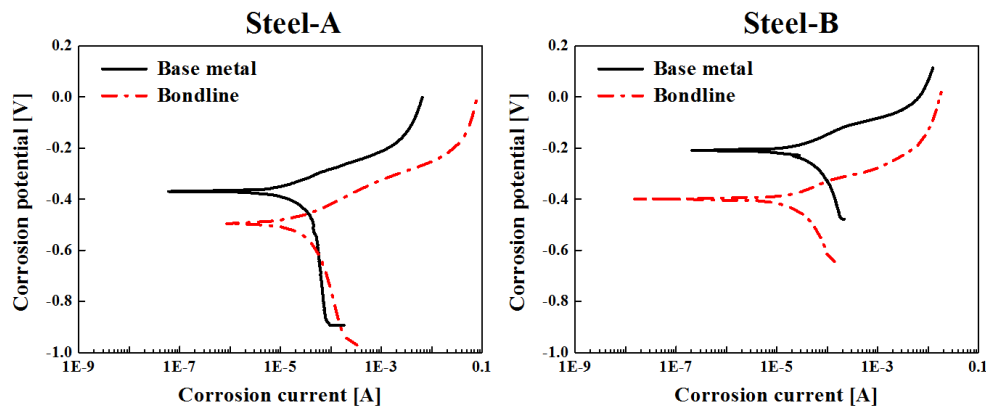


Fig. 6 Polarization diagram showing comparison between base metal and bond-line (a) Steel-A and (b) Steel-B.

Table 3 Electrochemical properties of ERW pipes from potentiodynamic polarization test

		E _{corr} (V)	I _{corr} (A)
Steel-A	Base metal	-0.368	6.74E-6
	Bondline	-0.496	9.80E-6
Steel-B	Base metal	-0.21413	1.65E-5
	Bondline	-0.40243	1.27E-5

inal specimen's thickness and the corroded specimen's thickness. Each test of the grooving corrosion sensitivity was repeated three times.

The electrochemical polarization tests of the base metal and the welding zone were done in 3.5 wt% NaCl solution at room temperature using the Versastat 3. A scanning rate was 3 mV/s with the reference electrode (solid) of Ag/AgCl/KCl (0.197 volts) during polarization curve measurement. Prior to testing, the exposed surface was ground with 100 – 1000 grit emery paper. Microstructures of the ERW steel pipes were examined by Optical microscope. Analysis of microstructures of base metal and bonding were carried out three times and then the average values of the ferrite grain size and amount of pearlite are noted down.

3. Results and discussion

Fig. 5 shows V-shaped corrosion grooves located at the center of the fusion zone in steel-A and steel-B ERW pipes. It indicates that the corrosion rate at the bondline is higher than that of the base metal. The grooving factor (α) and the band width (B.W.) of the specimens are also shown in the Fig. 5. It specifies that the average grooving

factor of steel-A is higher than that of steel-B pipe. Therefore, it can be said that steel-A pipe has high grooving corrosion sensitivity than steel-B. The electrochemical polarization potentials of the ERW pipe specimens immersed in 3.5 wt% NaCl were measured with respect to the reference electrode of Ag, AgCl/KCl. The potentials vs. current density plot in Fig. 6 shows that the current density decreases with increasing polarization potential, but after a certain potential, which is called the corrosion potential with respect to the reference electrode, the current density starts to increase. A comparison of corrosion behaviour of the bondline and the base metal can be obtained from Fig. 6 and Table 3. The corrosion potential and the corrosion current of the base metal and the bondline are different. In other words, the polarization curve

of the bondline is located below of the base metal. It indicates that there is an electrochemical kinetic difference between the bondline and the base metal of ERW steel pipes in corrosive environment. This kinetic difference in addition to galvanic coupling that develops due to differences in the corrosion potentials would accelerate selective corrosion in ERW pipes [2]. The potential in the bondline was consistently more negative and the high current density in the bonding than the base metal. As a result, the weld zone becomes more active than the base metal, which leads to the severe corrosion at the weld bondline as the welding zone experiences higher corrosion rates than the base metal. Furthermore, the difference in current density of the base metal and the bondline of steel-B is lower than in steel-A. So, it can infer that the bondline

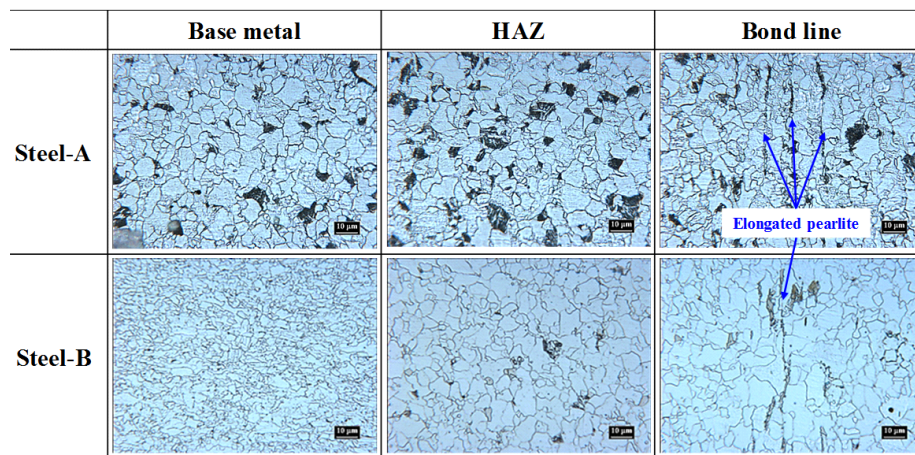


Fig. 7 Microstructures of the base metal, HAZ and the bondline.

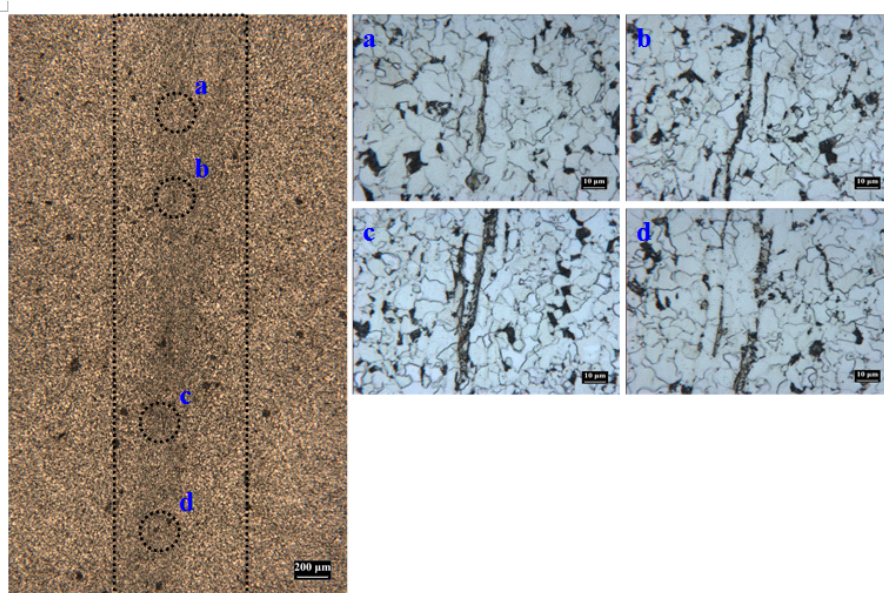


Fig. 8 Detailed microstructure of bondline in Steel-A.

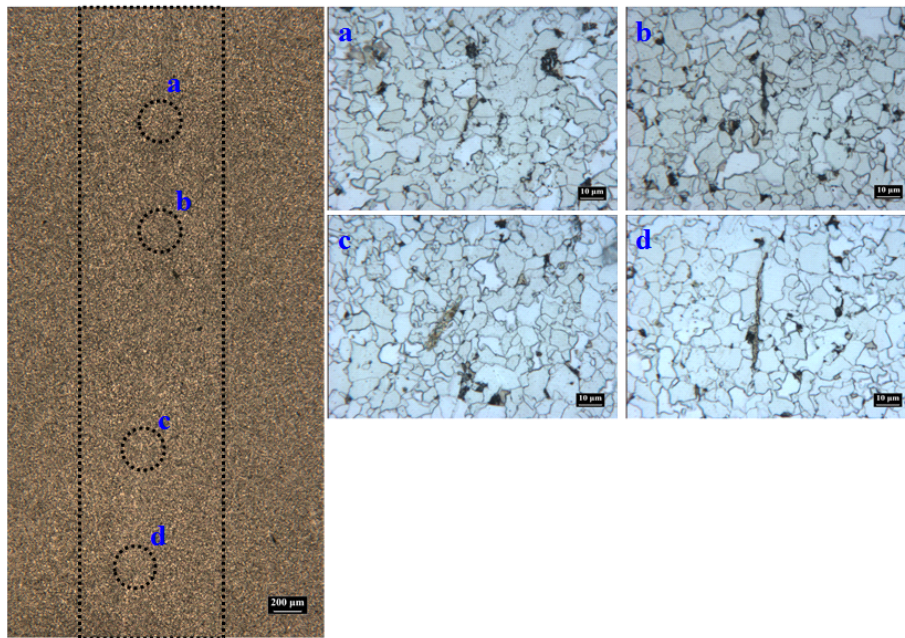


Fig. 9 Detailed microstructure of bondline in Steel-B.

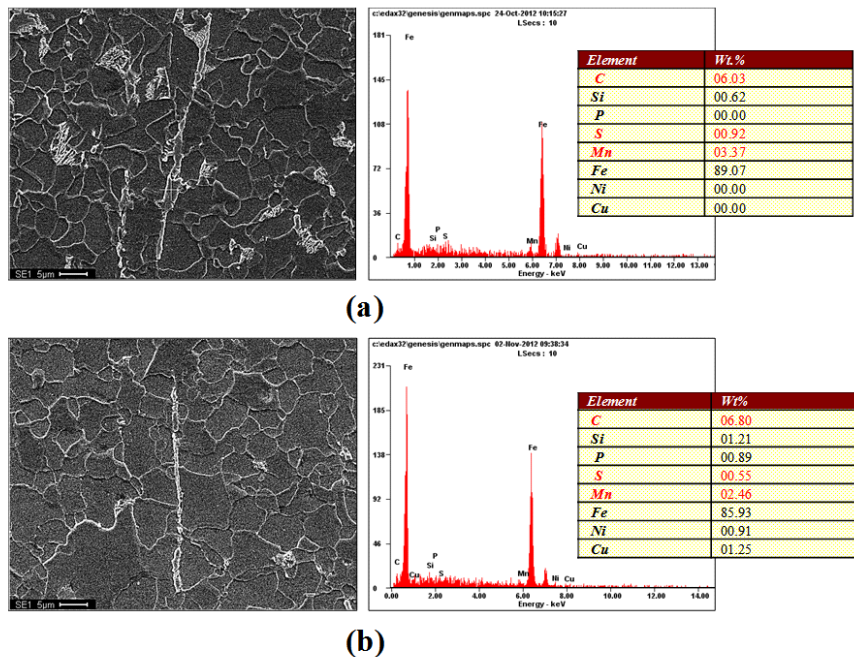


Fig. 10 SEM-EDS analysis at the bondline: (a) Steel-A; (b) Steel-B.

of steel-A exhibits faster corrosion rate than the bondline of steel-B.

Fig. 7 shows the comparison of microstructure of the base metal, HAZ and the bondline of the two ERW pipes. A detailed microstructure of the bondline of the two pipes are provided in Fig. 8 and Fig. 9. The microstructure of bondline is composed of coarse polygonal ferrite grains

and few elongated pearlites. The elongated pattern is mainly concentrated in the center of the bond area. Moreover, a higher volume of the elongated structure is observed in steel-A than in steel-B. Detailed SEM-EDS analysis as shown in Fig. 10 reveals that the elongated pearlite is associated with the oxides and sulfides of Mn-Si. These structures are formed during the welding

Table 4 Measurement of avg. ferrite grain size and pearlite volume fraction

	Steel-A		Steel-B	
	Base Metal	Bondline	Base Metal	Bondline
Avg. Ferrite grain size	120 μm	84 μm	53 μm	115 μm
Pearlite volume fraction	4.9 %	6.6 %	0.8 %	2.2 %

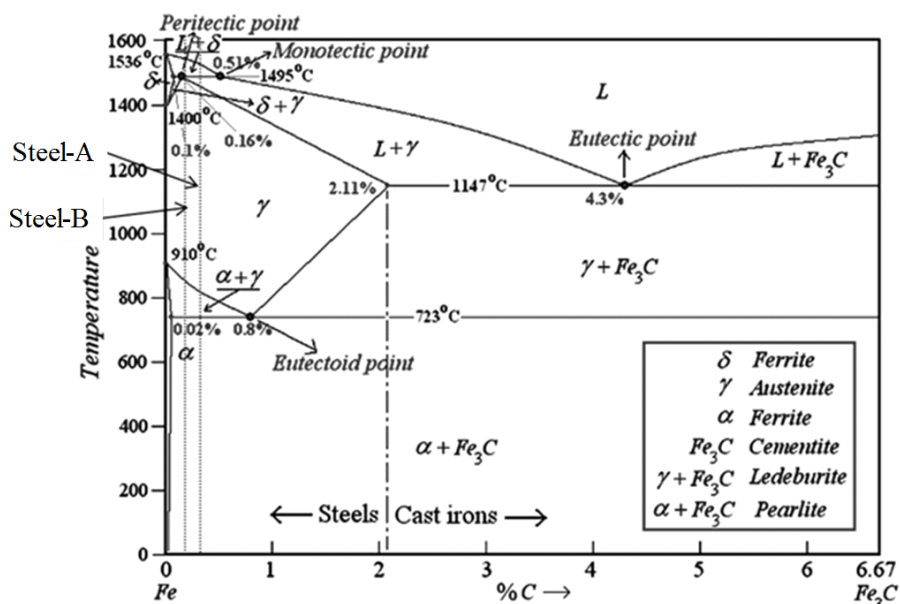


Fig. 11 Iron – Iron carbide phase diagram.

operation as a result of high temperature reaction of Mn-Si with S and O, and a subsequent expulsion on the forging action. Iron-iron carbide phase diagram, in Fig. 11, is used to explain the microstructural features of the investigated steels. From phase diagram, it is evident that steel-B consists of less pearlite volume fraction compared to steel-A. Comparison between steel-A and steel-B in terms of ferrite grain size and the pearlite volume fraction is shown in Table 4. The lower pearlite volume fraction is proportionate to the lower carbon content in steel-B, whereas the grain size is most likely obtained by control of the welding parameters and the heat treatment process, noting the absence of grain refining elements. The grains of the base metal steel-B are finer than that of steel-A. Also, elongated pearlite is observed in the bondlines of both the steels. Selective and localized corrosion tests and microstructural observations show that the grooving corrosion existed in the ERW pipes and appeared only in the welding zone. Generally, the localized and general corrosion rates vary slightly between different carbon steels, but the microstructure has some effect on the corrosion [4]. Carbon content determines the microstructure of steel, including the base metal and the weldment, according to

the Fe-Fe₃C phase diagram in Fig. 11. The welding parameters and the heat treatment process can modify the microstructure. Steel-A has higher carbon content than steel-B. Again, from the welding parameters in Table 2, steel-A has lower heat input during welding than steel-B. Therefore, it can be the reason of smaller ferrite grains and more pearlite is present at the weld zone of steel-A compared to steel-B. The steel with coarser ferrite microstructure performed better in terms of the average corrosion [5] and the ferrite microstructure showed the lowest corrosion rate [6]. In the steel with ferritic-pearlitic microstructure, with pearlite consisting of ferrite and cementite, the cementite acts as a cathode in an electrolyte while the ferrite phase corrodes preferentially [7,8]. The welded pipes had higher risk of localized corrosion due to existence of pearlites in the welding zone. In order to reveal the process of the grooving corrosion, the current density, including the base metal and the bondline, was recorded at the polarization test. As there is a significant change in current densities between the base metal and the bondline, the corrosion rate is faster at the bondline due to higher current density. In steel-A pipe the difference in current densities is more prominent than the steel-B.

Also, the corrosion potential at the bondline is often lower than the base metal due to the existence of pearlite. It may be deduced from these results that the grooving corrosion occurs due the presence of more pearlite at the weld zone. Generally, in mild and low alloy steels, small amount of Cr, Ni, Cu and Ca influenced the corrosion behavior and the corrosion rate tended to decrease as the result of alloying [9,10]. Therefore, the alloying elements should improve the resistance of steels to corrosion. For ERW pipes, there is a difference of alloying element between the base metal of steel-A and steel-B. Presence of V, Nb, Cr and Ni the base metal of SR70 makes it more corrosion resistant than the base metal of NS65 [11]. Therefore, steel-B pipe has less sensitivity of the grooving corrosion than steel-A.

4. Conclusion

Investigation was done on the grooving corrosion performance of X65 grade Non-Sour Service (steel-A) and X70 grade Sour gas resistant (steel-B) steel pipelines and the following conclusions were drawn. V-shaped corrosion groove was formed at the center of the fusion zone in both steel-A and steel-B ERW pipes, as the corrosion rate of the bondlines is higher than that of the base metal.

Higher volume fraction of pearlite in the bondline was responsible for the higher corrosion rate at the bondline of both the steels.

References

1. C. Kato, Y. Ootoguro, S. Kado, and Y. Hisamatsu, *Corros. Sci.*, **18**, 61 (1978) .
2. R. Wang and S. Luo, *Corros. Sci.*, **68**, 119 (2013).
3. Z. Bi, R. Wang, and X. Jing, *Corros. Sci.*, **57**, 67 (2012).
4. A. A. Azim, and S. H. Sanad, *Corros. Sci.*, **12**, 313 (1972).
5. D. Clover, B. Kinsella, B. Pejicic, and R. De Marco, *J. Appl. Electrochem.*, **35**, 139 (2005).
6. M. A. Lucio-Garcia, J. G. Gonzalez-Rodriguez, M. Casales, L. Martinez, J. G. Chacon-Nava, M. A. Neri-Flores, and A. Martinez-Villafañe, *Corros. Sci.*, **51**, 2380 (2009).
7. J. Sánchez, J. Fullea, C. Andrade, J. J. Gaitero, and A. Porro, *Corros. Sci.*, **50**, 1820 (2008).
8. F. Kellou-Kerkouche, A. Benchettara, and S. Amara, *Mater. Chem. Phys.*, **110**, 26 (2008).
9. Y. S. Choi, J. J. Shim, and J. G. Kim, *J. Alloy. Compd.*, **391**, 162 (2005).
10. R. E. Melchers, *Corros. Sci.*, **46**, 1669 (2004).
11. L. R. Bhagavathi, G. P. Chaudhari, and S. K. Nath, *Mater. Design*, **32**, 433 (2011).